RSC Advances

COMMUNICATION

View Article Online
View Journal | View Issue



Cite this: *RSC Adv.*, 2016, **6**, 80666

Received 9th May 2016
Accepted 15th August 2016

DOI: 10.1039/c6ra12020b

www.rsc.org/advances

# Peculiarities of the magneto-optical response in dispersions of anisometric pigment nano-particles†

A. Eremin,*[a] Y. Geng,[a] R. Stannarius,[a] T. Ostapenko,[b] P. K. Challa,[c] J. T. Gleeson,[c] A. Jákli[d] and S. Klein[e]

We demonstrate an unusually strong magneto-optical response of elongated plate-shaped pigment particles in magnetic fields ranging from 0 to 25 T. In a weak field, the particles align perpendicular to the field and the dispersions exhibit the Cotton–Mouton effect. In a strong magnetic field, the magneto-optical behaviour is nonlinear and cannot be explained by a simple model of non-interacting diamagnetic rods in a thermal equilibrium. We also demonstrate that the addition of a small amount of magnetic particles results in a complex magneto-optical response, where the particles align parallel to a weak magnetic field and perpendicular to a strong one.

The study of colloidal suspensions under the action of a magnetic field dates back to the beginning of the 20th century. In 1901, J. Kerr reported a magnetically induced birefringence in suspensions of magnetite.[1] In pure fluids, weak magnetically induced birefringence was discovered by Cotton and Mouton.[2] Yet, development of colloidal materials for efficient magneto-optical applications requires a high susceptibility to the magnetic field and a strong optical response. The latter can be achieved using anisometric particles with anisotropic optical properties in combination with super-paramagnetic fluids, such as ferrofluids. Ferrofluids have exceptional magnetic properties, which makes them interesting for applied research. However, strong light absorption in ferrofluids restricts their potential for magneto-optical applications. Lemaire *et al.* demonstrated magnetic-field-induced birefringence in suspensions of colloidal goethite (α-FeOOH) nano-rods.[3–5] These anisometric particles demonstrated not only a strong response to an external magnetic field, but they also exhibited an orientationally ordered nematic liquid crystal phase. Another interesting feature of this system is the reorientation of the rods at a high field strength. Goethite nano-rods align along the field direction below 0.35 T and perpendicular to the field above 0.35 T. Most other suspensions of anisometric particles studied, such as fd and tobacco mosaic viruses, gibbsite platelets, and plate-shaped biological membranes and cells, behave as diamagnetic and do not exhibit any appreciable magneto-optic effects at low and moderate magnetic fields.[6–11] Yet, a combination of anisotropic soft non-magnetic materials with enhanced optical properties, such as liquid crystals and magnetic fluids, opens up the possibilities to develop novel multifunctional and multiferroic materials.[12,13]

In this paper, we report our studies of magneto-optical properties of dispersions of dichroic elongated plate-shaped pigment particles. In previous studies, we showed that this system displays a rich variety of phenomena, such as mesophase behaviour, electro-optical response, and pattern formation in electric fields.[14–16] At small volume fractions, these dispersions exhibit an isotropic and a paranematic state. The latter is distinguished by a strong optical response to an external electric field. At volume fractions above 13.5 v%, the suspension shows a spontaneous orientationally ordered phase. We characterise the magneto-optical response of those dispersions in the isotropic and paranematic states, and also demonstrate that, addition of a small amount of the ferromagnetic nanoparticles drastically enhances the magneto-optical response.

We used suspensions of Permanent Rubine, a yellow shade calcium salt red pigment consisting of platelets with an average length of 180 nm ± 81 nm, average width of 64 nm ± 22 nm and an average thickness of 12 nm ± 8 nm. High-field studies were made on the dispersions of the Pigment Red 176, a blue shade benzimidazolone pigment. One of its commercially available forms is Novoperm Carmine HF3C (Clariant, Frankfurt am Main, Germany), used as received where the primary particles are elongated platelets with a mean length of 230 nm ± 70 nm

[a]Otto-von-Guericke-Universität Magdeburg, FNW/IEP/ANP, Postfach 4120, 39016 Magdeburg, Germany. E-mail: alexey.eremin@ovgu.de
[b]Max Planck Institute for Dynamics and Self-Organization (MPIDS), Am Faßberg 17, 37077 Göttingen, Germany
[c]Department of Physics, Kent State University, Kent, OH, 44242, USA
[d]Liquid Crystal Institute, Kent State University, Kent, OH 44242, USA
[e]HP Laboratories, Long Down Avenue, Stoke Gifford, Bristol BS34 8QZ, UK

† Electronic supplementary information (ESI) available. See DOI: 10.1039/c6ra12020b

and a mean width of 46 nm ± 20 nm and thickness 17.3 nm ± 8 nm. All suspensions were prepared in a nonpolar solvent, dodecane (Sigma-Aldrich, Hamburg, Germany, used as received) as described in ref. 15 and 16. We added Solsperse 11200 (Lubrizol, Brussels, Belgium, used as received) as a dispersant. Two-component mixtures of pigment and ferromagnetic particles were prepared by mixing the pure pigment suspension with small amounts of an oil-based commercial ferrofluid, APG935 (FerroTech GmbH, Germany). The ferrofluid contains magnetite nanoparticles with average diameter of about 10 nm suspended in hydrocarbons. The surfactant layer thickness can be estimated to be about 2 nm. The mixture was sonicated for 30 min and no traces of phase separation were found over several months.

A polarised laser beam traverses a 25 μm sample cell filled with the colloidal suspension. Samples were held within the bore of a split-helix resistive magnet at the National High Magnetic Field Laboratory. We used the Voigt geometry in which the light direction is perpendicular to the magnetic field, and the polariser and analyser are oriented at ±45° (to the field direction), respectively. In this geometry, we use the photoelastic modulator (PEM) technique[17–19] to measure optical anisotropy (birefringence and dichroism). The fast axes of the sample and PEM were parallel to the magnetic field. The modulator introduces a time-dependent optical phase shift $\phi(t) = A \sin(\omega t)$. The transmitted light intensity was recorded using a photodetector with the signal measured simultaneously by both a lock-in amplifier and DC multimeter. Three separate Fourier amplitudes of the time dependent photodetector signal are recorded, $V_{DC}$, $V_\omega$ and $V_{2\omega}$. The value of the linear dichroism LD is given by LD $= V_\omega/V_{DC}$ and birefringence $\Delta n = \frac{\lambda}{2\pi d}\arctan\left(\frac{V_\omega}{V_{2\omega}}\frac{J_2(A)}{J_1(A)}\right)$, where $\lambda = 632.8$ nm is the laser wavelength and $d$ is the cell thickness. $J_n(A)$ is the Bessel function of the first kind of integer order $n$.[20]

Dispersions of the pigment particles only were found to be diamagnetic in weak magnetic fields. At low volume fraction $\varphi$ of pigments, where the dispersion is isotropic, a small birefringence could be induced by the magnetic field. Below 1 T, the birefringence exhibits a quadratic dependence on the applied magnetic field **B**, typical for the Cotton–Mouton effect (Fig. 1a). The birefringence is negative, as demonstrated in an experiment with a quarter-wave plate. When the slow optical axis of the quarter-wave plate, inserted together with the sample, is parallel to the magnetic field **B**, the retardation is decreasing (Fig. 1b). This corresponds to the subtractive birefringence of the sample. The retardation increases when the retarder is inserted perpendicular to **B**. Assuming that the pigment particles have a larger birefringence along their long axes, we can conclude that the particles align perpendicular to the magnetic field *i.e.*, the birefringence is negative.

The slope $\Delta n/B^2$ of $\Delta n/(B, \varphi)$ increases with the particle volume fraction. From this, we find the Cotton–Mouton constant: $K_{CM} = \Delta n/\lambda B^2$, where $\lambda = 632.8$ nm is the wavelength of the laser and $B$ is the magnetic field strength. Fig. 2 shows a nearly linear dependence of $K_{CM}(\varphi)$ on the volume fraction $\varphi$. This result is in stark contrast with results for gibbsite particles.[6] First, the Cotton–Mouton constant of our pigment dispersions is nearly two orders of magnitude larger than that of gibbsite. The pigment particles are formed by organic molecules with extended conjugated bindings. Additionally, the nano-crystals are cut in directions of the crystallographic planes and have a strong shape anisometry. This may be responsible for a strong optical response such as birefringence and the dichroism.

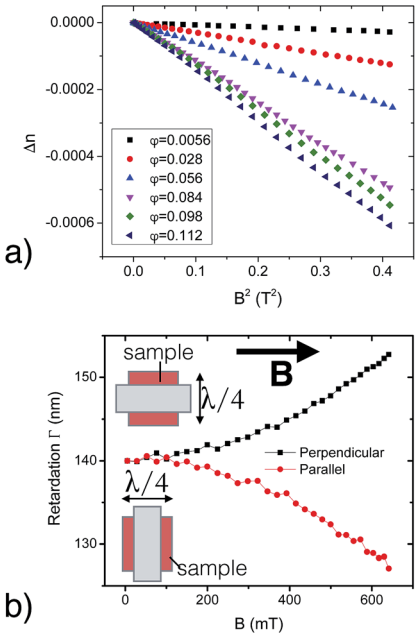


Fig. 1 Magnetic-field-induced birefringence of Permanent Rubine: (a) $\Delta n$ measured for various volume fractions. The slope $\Delta n/B^2$ is nearly proportional to the volume fraction $\varphi$ of pigments. The retardation decreases when a quarter-wave retarder is inserted with a slow optical axis parallel to $B$, and increases otherwise (b) (for $\varphi = 0.056$), showing that the birefringence is negative.

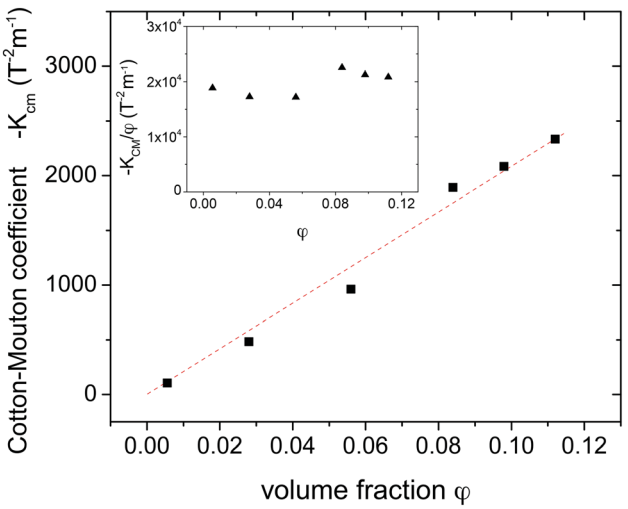


Fig. 2 Cotton–Mouton coefficient as a function of the volume fraction of the pigment particles of Permanent Rubine. The inset shows the reduced constant $K_{CM}/\varphi$.

Secondly, the reduced Cotton–Mouton constant $K_{CM}/\varphi$ is almost independent of volume fraction (see inset in Fig. 2) within experimental accuracy, *i.e.*, show the absence of a divergent behaviour close to the transition into an orientationally ordered phase at $\varphi_m = 0.135$ (Fig. 2).

The behaviour of Novoperm Carmine in strong magnetic fields is shown in Fig. 3. The quadratic growth of $\Delta n(B)$ at small $B$ transforms into a slower saturation-type behaviour at large $B$. No hysteresis was found on increasing/decreasing ramps of the magnetic field. Unexpectedly, at low volume fraction $\varphi = 0.0056$, $\Delta n$ shows a small plateau at $B \approx 3$ T. To describe this behaviour, we consider that the birefringence is proportional to the orientational order parameter $S = \left\langle \frac{3}{2}\cos^2(\theta) - \frac{1}{2} \right\rangle$ of the rods, where $\theta$ is the angle between a particle and a preferred direction (magnetic field) and the brackets stand for the ensemble average over all particles. Neglecting interparticle interactions, the ensemble average can be calculated using Boltzmann statistics. The orientation-dependent magnetic energy of the particle is $U_m(\theta) = -\Delta\chi_p B^2 \cos^2\theta/2$, where $\Delta\chi_p = \chi_{p\parallel} - \chi_{p\perp}$ is the effective anisotropy of the diamagnetic particle susceptibility[8] containing molecular and shape-anisotropy contributions, $\theta$ is the angle between the particle long axis and the magnetic field. The particle susceptibility is determined by the diamagnetic susceptivity of the material $\Delta\chi$ and the particle volume $V$ as $\Delta\chi_p = \Delta\chi/\mu_0$.

Designating $\frac{\Delta\chi_p}{2k_bT}$ by $\beta$, we obtain:

$$\langle \cos^2\theta \rangle = \frac{\int_0^\pi e^{\beta B^2 \cos^2\theta} \cos^2\theta \sin\theta d\theta}{\int_0^\pi e^{\beta B^2 \cos^2\theta} \sin\theta d\theta} \quad (1)$$

The integrals can be evaluated analytically and yield the order parameter:

$$S(B^2) = \frac{3}{2}\left( -\frac{1}{B\sqrt{\pi\beta}} \frac{e^{-\beta B^2}}{\mathrm{erf}(\sqrt{\beta}\,B)} + \frac{1}{2\beta B^2} \right) - \frac{1}{2} \quad (2)$$

In the low-field limit $B \to 0$, the order parameter $S$ in eqn (2) exhibits a quadratic dependence on $B$: $S \approx \frac{2}{15}\frac{\Delta\chi}{k_bT}B^2$ (Cotton–Mouton effect). In the high-field limit, $B \to \infty$, the orientational order parameter $S$ approaches $-0.5$ and the birefringence tends to its saturation value $\Delta n_s$. We assume a linear dependence of the birefringence on the order parameter $\Delta n = -2\Delta n_s S$, where $\Delta n_s$ is the saturation birefringence which depends on the particle properties. The model in eqn (2), however, fails to satisfactory describe the experimental data in high fields (Fig. 3). The saturation is reached at much higher fields than expected from the analysis of the quadratic trend at low fields. A closer examination of the curves reveals two contributions to the birefringence $\Delta n = \Delta n_{s,1} S(B, \Delta\chi_{p1}) + \Delta n_{s,2} S(B, \Delta\chi_{p2})$. One susceptibility is about one to two orders of magnitude smaller than the other one. Satisfactorily fits with the two-component model are shown in Fig. 3. Both fits give comparable susceptibilities for the two different components $\Delta\chi_{p1} = 5.4 \times 10^{-21}$ J T$^{-2}$ and $\Delta\chi_{p2} = 6.0 \times 10^{-23}$ J T$^{-2}$ for $\varphi = 0.0056$ J T$^{-2}$ and $\Delta\chi_{p1} = 1.6 \times 10^{-21}$ J T$^{-2}$ and $\Delta\chi_{p2} = 7.9 \times 10^{-23}$ J T$^{-2}$ for $\varphi = 0.084$. Susceptibility values in the order of magnitude of $10^{-21}$ J T$^{-2}$ are astonishingly high. They are about two orders of magnitude higher than in the gibbsite system reported in ref. 6 and along with strong optical anisotropy of pigment particles are responsible for an appreciable magneto-optical response even at $B < 1$ T.

It is not clear, however, what is responsible for the second component of the optical response. It can arise from the surfactant present in the solution. Alternatively, the two components may be attributed to single particles and their clusters. At high volume fractions, the inter-particle correlations cannot be neglected any more and the approximation in eqn (2) is not valid any more.

The addition of a small amount of magnetic nanoparticles, such as those in ferrofluids, significantly increases the magneto-optical response. We studied it by measuring the linear dichroism (LD) at various volume fractions of the magnetic particles in the pigment/ferrofluid binary mixtures (Fig. 4a). The magnetic field dependence of the linear dichroism is proportional to the order parameter $S$, so it is also indicative of the degree of orientational order of the particles. In weak fields, $B < 1$ T, the sign of LD is positive. This indicates that the particles align along the magnetic field direction (Fig. 4b). At stronger fields, however, LD decreases and changes its sign. Such behaviour can be attributed to a competition between the diamagnetic interactions of the pigment particles and superparamagnetic behaviour of the ferrofluid. In low magnetic fields, the linear interactions between the ferromagnetic particles and the field dominate. The magnetic particles form small anisometric aggregates (fragments of chains). Their alignment is sterically transferred to the non-magnetic component – the pigment particles. The mechanism of this alignment transfer is described by the Lekkerkerker–Onsager theory[21,22] and was

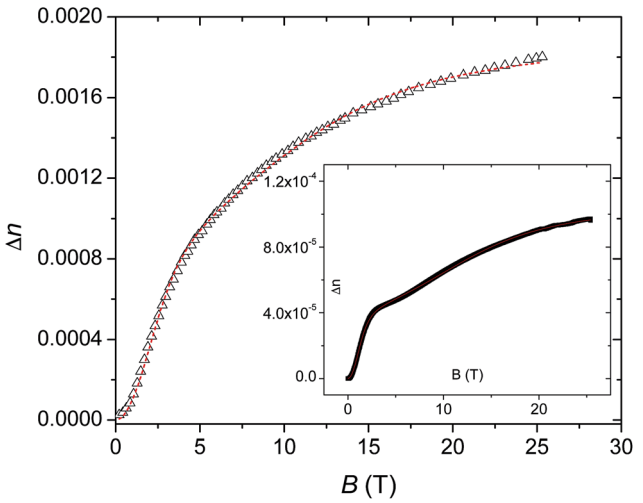


Fig. 3 Birefringence *vs.* magnetic field of a dispersion of Novoperm Carmine with $\varphi = 0.084$ confined in a 25 μm thick glass cell, and $\varphi = 0.0056$ measured in a 1 mm thick cuvette is shown in the inset. The solid lines are fits with a two-component model discussed in the text.

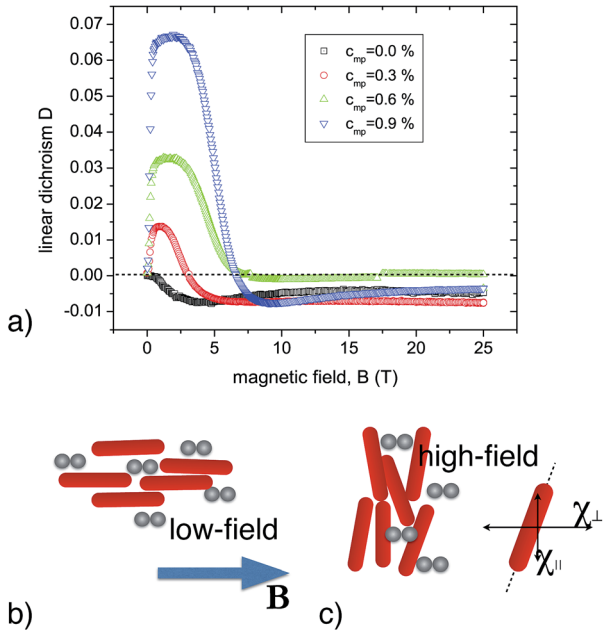


Fig. 4 (a) Linear dichroism in binary mixtures of the pigment particles (Novoperm Carmine) with varying volume fraction $C_{mp}$ of the ferromagnetic nanoparticles APG935; (b) scheme illustrating the alignment of small magnetic-particle chains (grey) aligning the non-magnetic pigment rods (red) in a weak magnetic field; (c) in a high field, the diamagnetic force dominates and aligns the pigment particles nearly perpendicular to the field. The principal axes of the effective diamagnetic anisotropy are ensemble averaged and given by the mean direction of the pigment particles.

demonstrated by Reznikov *et al.* for binary mixtures of non-magnetic $V_2O_5$ rods with magnetic $Fe_3O_4$ nanoparticles.[23] Unexpectedly, the (negative) saturation value of the dichroism in a high field $D_h$ is much smaller than the (positive) maximum $D_l$ at intermediate fields. In the case of perfect parallel/perpendicular alignments, the ratio of $D_h/D_l$ should be $-1/2$, *i.e.* equal to the ratio of the order parameters in the two states. A possible explanation of the experimental observations would be that the directions of the principle axes of the susceptibility tensor $\chi$ are not parallel to the symmetry axes of the pigment particles but make a finite angle between them. As a result, the particles will not perfectly align perpendicular to $B$ (see Fig. 4c), which could lead to a reduction of $|D_h|$.

In summary, we have investigated the magneto-optical properties of suspensions of the elongated plate-shaped dichroic particles with and without the addition of spherical ferromagnetic nanoparticles. The pigment dispersions only showed an unusually strong field-induced birefringence, which is even stronger than that in colloidal dispersions of goethite platelets. The crystallite rods of both Permanent Rubine and Novoperm Carmine align perpendicular to the magnetic field, suggesting a negative diamagnetic anisotropy. This can be attributed both to an unusually high optical anisotropy of the pigment nano-particles, which is determined by birefringence and enhanced by the linear dichroism, and a strong anisotropy of the diamagnetic susceptibility. The alignment of the particles is substantially modified when a small amount of ferromagnetic particles is added. Subsequently, the pigment rods align parallel to the field at low magnetic fields, and perpendicular to it in strong fields, yielding substantial magnetically induced dichroism.

## References

1 J. Kerr, *Report of the Annual Meeting of the British Association for the Advancement of Science*, 1901, p. 568.
2 A. Cotton and H. Mouton, *C. R. Hebd. Seances Acad. Sci.*, 1905, **141**, 349.
3 B. J. Lemaire, P. Davidson, J. Ferré, J.-P. Jamet, D. Petermann, P. Panine, I. Dozov, D. Stoenescu and J.-P. Jovilet, *Faraday Discuss.*, 2005, **128**, 271–283.
4 B. J. Lemaire, P. Davidson, D. Petermann, P. Panine, I. Dozov, D. Stoenescu and J. P. Jolivet, *Eur. Phys. J. E*, 2004, **13**, 309–319.
5 B. J. Lemaire, P. Davidson, J. Ferré, J. P. Jamet, D. Petermann, P. Panine, I. Dozov and J. P. Jolivet, *Eur. Phys. J. E*, 2004, **13**, 291–308.
6 D. van der Beek, A. V. Petukhov, P. Davidson, J. Ferré, J. P. Jamet, H. H. Wensink, G. J. Vroege, W. Bras and H. N. W. Lekkerkerker, *Phys. Rev. E*, 2006, **73**, 041402.
7 S. Fraden, G. Maret and D. Caspar, *Phys. Rev. E: Stat. Phys., Plasmas, Fluids, Relat. Interdiscip. Top.*, 1993, **48**, 2816–2837.
8 A. Yamagashi, T. Takeuchi, T. Hagashi and M. Date, *Phys. B*, 1992, 523–526.
9 H. Nakamura and K. Okano, *Phys. Rev. Lett.*, 1983, **50**, 186–189.
10 J. Torbet and G. Maret, *Biopolymers*, 1981, **20**, 2657–2669.
11 N. E. Geacintov, F. Van Nostrand, M. Pope and J. B. Tinkel, *Biochim. Biophys. Acta*, 1971, **226**, 486–491.
12 A. Mertelj, D. Lisjak, M. Drofenik and M. Copic, *Nature*, 2014, **504**, 237–241.
13 M. Kaczmarek, O. Buchnev and I. Nandhakumar, *Appl. Phys. Lett.*, 2008, **92**, 103307.
14 K. May, R. Stannarius, S. Klein and A. Eremin, *Langmuir*, 2014, **30**, 7070–7076.
15 R. J. Greasty, R. M. Richardson, S. Klein, D. Cherns, M. R. Thomas, C. Pizzey, N. Terrill and C. Rochas, *Philos. Trans. R. Soc., A*, 2013, **371**, 20120257.
16 A. Eremin, R. Stannarius, S. Klein, J. Heuer and R. M. Richardson, *Adv. Funct. Mater.*, 2011, **21**, 402.
17 J. C. Kemp, *J. Opt. Soc. Am.*, 1969, **59**, 950–953.
18 K. W. Hipps and G. A. Crosby, *J. Phys. Chem.*, 1979, **83**, 555–562.
19 B. Wang and T. C. Oakberg, *Rev. Sci. Instrum.*, 1999, **70**, 3847–3854.
20 I. Musevic, R. Blinc and B. Žekš, *The Physics of Ferroelectric and Antiferroelectric Liquid Crystals*, World Scientific Publishing Company Incorporated, 2000.
21 H. N. W. Lekkerkerker, P. Coulon, R. Van Der Haegen and R. Deblieck, *J. Chem. Phys.*, 1984, **80**, 3427.
22 G. J. Vroege and H. N. W. Lekkerkerker, *Rep. Prog. Phys.*, 1992, **55**, 1241–1309.
23 S. Kredentser, O. Buluy, P. Davidson, I. Dozov, S. Malynych, V. Reshetnyak, K. Slyusarenko and Y. Reznikov, *Soft Matter*, 2013, **9**, 5061.